A Porphyrin Embedded in DNA

Kurt Berlin, Rishi K. Jain, Matthew D. Simon, and Clemens Richert*

Department of Chemistry, Tufts University, Medford, Massachusetts 02155

Received September 30, 1997

Oligodeoxynucleotides containing an alkylporphyrin linked to the phosphate groups of DNA via oxypropyl chains have been synthesized. To our knowledge, these are the first porphyrin−nucleic acid conjugates bearing the porphyrin embedded in the backbone of DNA. Chain assembly was achieved by automated solid-phase synthesis using a dimethoxytrityl-protected porphyrin phosphoramidite and standard DNA building blocks. The thermal stability of duplexes involving the octadecamer 5′-CGCGCCTTC-P-CATTGCGG-3′, where -P- denotes the porphyrin, was found to depend on the sequence of the complementary strand. A duplex where a thymidine residue in the complementary strand faces the porphyrin gives a higher melting point than duplexes bearing an abasic site or a dT_3 loop at this position. Duplex formation is accompanied by 180% hypochromicity at 501 nm, and other spectral changes unprecedented in porphyrinoids interacting with nucleic acids. Footprinting with nuclease S1, together with CD spectropolarimetry, indicates that the alkylporphyrin is embedded in a B-type duplex, with highly nuclease-sensitive phosphates only in the local environment of the porphyrin. Peak shifts in the NMR spectrum of the porphyrin-containing duplex, together with fluorescence data, point toward an interaction between the porphyrin and the stacked nucleobases. Porphyrin-containing DNA- and RNA-duplexes, conveniently prepared with the porphyrin phosphoramidite described here, are expected to be valuable for photochemical and electron-transfer studies, as well as potential cofactor-using nucleic acid-based enzymes which could have had a role in prebiotic evolution.

Introduction

Porphyrin−nucleic acid interactions have been studied for some time. Since the early reports by Fiel and collaborators,[1] a variety of porphyrins and their metal derivatives have been shown to bind to single[2]- and double-stranded DNA,[3] and to folded RNA sequences.[4] The resulting complexes have been employed for studies on electron transfer through DNA,[5] nucleic acid-directed porphyrin aggregation,[6] and the potential DNA damage induced by sensitizers employed for photodynamic therapy of neoplastic tissue.[7,8] Common structural features of nucleic acid-binding porphyrins are a positive charge and bulky aryl substituents in the meso-positions. Recently, the first X-ray crystal structure of a complex between such a cationic tetraarylporphyrin and a DNA hexamer duplex was solved.[9] In this complex, for whose structural characteristics the term "hemiintercalation" was coined, the overwhelming number of observed contacts were found between the pyridyl ligands and the DNA but not between the porphyrin and the DNA. In fact, the porphyrin macrocycle does not stack with adjacent nucleobases. Besides van der Waals contacts, a number of electrostatic interactions between the pyridyl groups and the DNA phosphates were found to stabilize the complex, in agreement with earlier in solution studies, demonstrating that binding can be disrupted by increasing the salt concentration.[10]

While this X-ray structure helps to end earlier speculations that the intercalation of tetraarylporphyrins into DNA could involve rotation of the aryl substituents to a coplanar state, it leaves open the question whether the porphyrin macrocycle *by itself* is capable of binding to nucleic acids. To address this question, we set out to synthesize porphyrin−DNA conjugates where a porphyrin is held by two short tethers such that it can either interact with neighboring nucleic acids or remain unbound in solution. This required the development of a porphyrin building block suitable for incorporation of the porphyrin in the backbone of a DNA strand. Here we report the synthesis of such a building block and the conjugates resulting from its incorporation in oligodeoxynucleotides, together with a preliminary account of spectroscopic studies on the interactions of the tethered alkylporphyrin to single- and double-stranded DNA.

(1) (a) Fiel, R. J.; Howard, J. C.; Mark, E. H.; Datta-Gupta, N. *Nucleic Acids Res.* **1979**, *6*, 3093−3118. (b) Fiel R. J.; Munson, B. R. *Nucleic Acids Res.* **1980**, *8*, 2835−2842.

(2) (a) Carvlin, M. J.; Fiel, R. J. *Nucleic Acids Res.* **1983**, *11*, 6121−6139. (b) Pasternack, R. F.; Brigandi, R. A.; Abrams, M. J.; Williams, A. P.; Gibbs, E. J. *Inorg. Chem.* **1990**, *29*, 4483−4486.

(3) Selected references: (a) Pasternack, R. F.; Gibbs, E. J.; Villafranca, J. J. *Biochemistry* **1983**, *22*, 2406−2414. (b) Gibbs, E. J.; Maurer, M. C.; Zhang, J. H.; Reiff, W. M.; Hill, D. T.; Maliska-Blaskiewicz, M.; McKinnie, R. E.; Liu, H. Q.; Pasternack, R. F. *J. Inorg. Biochem.* **1988**, *32*, 39−65. (c) Sari, M. A.; Dupre, D. *Biochemistry* **1990**, *29*, 4205−4215. Other references cited in their specific context throughout the paper.

(4) (a) Foster, N.; Singhal, A. K.; Smith, M. W.; Marcos, N. G.; Schray, K. J. *Biochim. Biophys. Acta* **1988**, *950*, 118−131. (b) Birdsall, W. J.; Anderson, W. R., Jr.; Foster, N. *Biochim. Biophys. Acta* **1989**, *1007*, 176−183. (c) Celander, D. W.; Nussbaum, J. M. *Biochemistry* **1996**, *35*, 12061−12069.

(5) Brun, A. M.; Harriman, A. *J. Am. Chem. Soc.* **1994**, *116*, 10383−10393.

(6) Pasternack, R. F.; Collings, P. J. *Science* **1995**, *269*, 935−939 and references therein.

(7) Meunier, B. *Chem. Rev. (Washington, D.C.)* **1992**, *92*, 1411−1456.

(8) (a) Marzilli, L. G. *New J. Chem.* **1990**, *14*, 409−420. (b) Pass, H. I., *J. Natl. Cancer Inst.*, **1993**, *85*, 443−456.

(9) Lipscomb, L. A.; Zhou, F. X.; Presnell, S. R.; Woo, R. J.; Peek, M. E.; Plaskon, R. R.; Williams, L. D. *Biochemistry* **1996**, *35*, 2818−2823.

(10) Fiel, R. J. *J. Biomol. Struct. Dyn.* **1989**, *6*, 1259−1274.

(11) (a) Inhoffen, H. H.; Bliesener, C.; Brockmann, K. M., Jr. *Tetrahedron Lett.* **1966**, 3779−3783. (b) DiNello, R. K.; Dolphin, D. *J. Org. Chem.* **1980**, *45*, 5196−5204.

S0022-3263(97)01805-7 CCC: $15.00
Published on Web 02/06/1998

Scheme 1

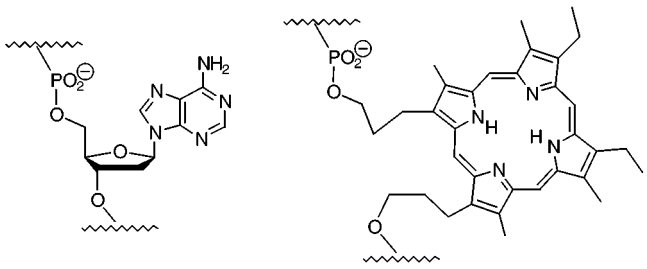

Results

The porphyrin to be embedded in DNA was designed to bear substituents similar to those found in porphyrins of biological importance. The design started from protoporphyrin IX. The polar propionic acid moieties were changed to the phosphate groups required for incorporation in the DNA backbone, and the vinyl groups were changed to ethyl groups to reduce sensitivity toward self-sensitized singlet oxygen.[11] The ethyl side chain is not uncommon among natural porphyrinoids formed from protoporphyrin, as seen e.g. in chlorophylls a and b. Finally, pyrrole ring II was "inverted"[12] to yield a symmetrical molecule, preventing the formation of regioisomers during synthesis. The resulting porphyrin (Scheme 1) and its potential metal complexes should reproduce the physicochemical properties of protoporphyrin and heme as closely as required. At the same time, the hydroxypropyl tethers were expected to provide the porphyrin ring with sufficient mobility to either intercalate in the DNA duplex or stay fully solvated. If intercalation or "hemiintercalation" would occur, the hydroxypropyl linkers would mimic the length of the ribose-"linkers" between nucleobases and phosphates in natural nucleotides. The desire to prepare a building block that could be used in standard phosphoramidite synthesis protocols for DNA and RNA led to porphyrin **1** (Scheme 2) as the key target of our synthesis.

Assembly of **1** started from known dipyrrylmethanes **2**[13] and **3**.[14] Tetraester **2** was converted to diol **4** through selective reduction with BH_3·THF in 68% yield after recrystallization. Hydrolysis and decarboxylation with hydrazine in refluxing aqueous solution furnished α,α′-unsubstituted dipyrrylmethane **5** as a yellowish oil that resisted crystallization. McDonald condensation[15] of dialdehyde **3** and **5** using *p*-toluenesulfonic acid[16] gave porphyrin **6** in 35% yield. Similar to a known porphycene dialcohol,[17] **6** displayed low solubility in most solvents and required tetrahydrofuran as eluant for column chromatography. The following protection of one hydroxyl group under statistical control necessitated a solvent mixture and elevated temperature for the same reason. Phosphitylation with bis(diisopropylamino)(β-cyanoethoxy)phosphine[18] afforded phosphoramidite **1** in good yield. The porphyrin building block was found to be more sensitive to hydrolysis than nucleoside phosphoramidites. Best results were obtained when **1** was precipitated from the reaction by addition of acetonitrile and cooling. Due to its low solubility in acetonitrile, **1** was dissolved in dichloromethane containing 0.2% triethylamine for solid-phase synthesis. To prevent precipitation of **1** in the DNA synthesizer, 10% dichloromethane was added to the tetrazole activator solution.

The methodology for assembly of hybrid oligomers was first tested with decamer **8** (Scheme 3). Chain assembly used standard DNA synthesis cycles, except that the coupling time was extended for the phosphitylation with **1**. Hybrid synthesis was then performed to produce to octadecamer **9**, whose solid phase assembly proceeded in ca. 50% overall yield, based on comparison of the first and the last trityl signal. Separation from the usual failure products was facilitated by the lipophilicity of the porphyrin "residue", which increased affinity for RP_{18} stationary phases considerably. In most cases, pure material could be obtained by a simple cartridge purification. The increased lipophilicity also led to an increased adsorption of the porphyrin-bearing oligonucleotides to polyethylene surfaces. When dilute aqueous solutions of **9** were lyophilized to dryness, redissolution was incomplete, unless at least 10 mM buffer solution was used.

Octadecamer **9** was annealed to a number of complementary DNA oligomers. The thermal denaturation of the resulting duplexes was measured by UV−vis spectrophotometry. The complementary strands contained either a "missing" nucleotide (**10**), an abasic site (**11**), a thymidine residue (**12**), a library of all four natural nucleotides (**13**), or a TTT-"bulge" (**14**) opposite the porphyrin residue (Scheme 3). As a control, melting of unmodified duplex **15**/**12** was measured under identical conditions. The complex between **9** and **12** had the highest melting point (T_m) among the porphyrin-containing duplexes, with a ΔT_m of −5.5 °C compared to the control (Figure 1). This duplex, with a thymidine residue opposite the porphyrin, also showed the sharpest melting

Scheme 2

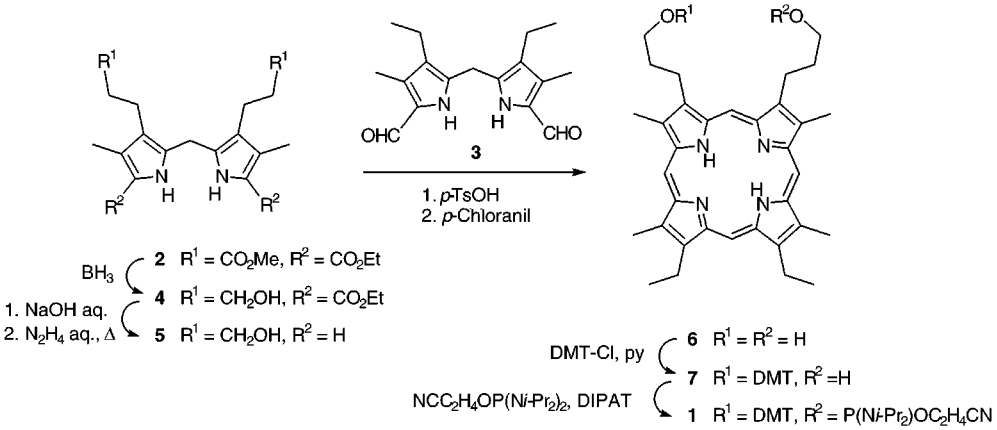

Scheme 3

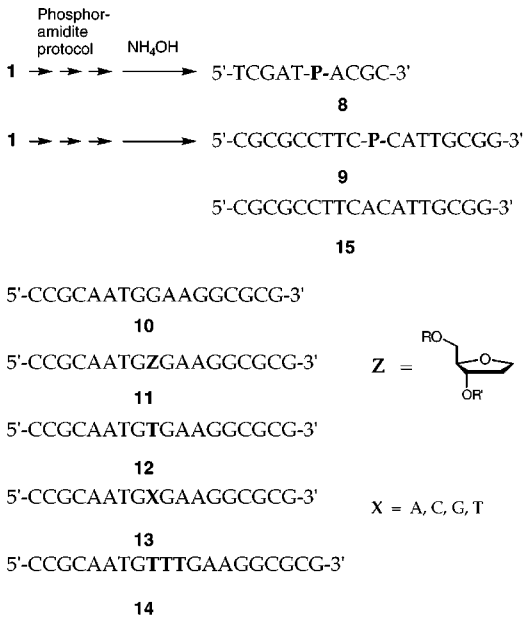

behavior, i.e., the most cooperative transition. Pronounced broadening of the melting transition was observed for duplex **9**/**14**, and particularly for duplex **9**/**11**, where hyperchromicity began ca. 30 °C below the melting point. This indicates that with the insertion of the TTT trinucleotide, or, to a lesser extent, with the interruption of base-stacking caused by an abasic site, some independent melting of the 3′- and 5′-regions may occur. Interestingly, melting points, as determined by the point of inflection of the temperature versus absorbance profile, still fell within ±2 °C for all but the TTT-bearing duplex (Table 1).

The highest melting complex, **9**/**12**, was studied in greater detail. The UV−vis spectrum of this duplex at room temperature revealed unexpectedly low intensities for the shortest and longest wavelength Q-band of the porphyrin. These bands showed strong hyperchromicity upon heating, whereas the absorption band at 563 nm lost intensity upon heating (Figure 2a). In the case of the Q-band at 501 nm, the hyperchromicity was 180% from 30 °C to 80 °C. At the same time, the maximum of the longest wavelength Q-band underwent a bathochromic shift from 608 to 617 nm. The latter value is similar to that found for bis(hydroxypropyl)porphyrin **6** in organic solvents (618 nm in CH_2Cl_2/MeOH 9:1), indicating that at elevated temperatures, where the two strands are dissociated, the porphyrin absorbs like that of the unconjugated control compound. The Sôret or B-band at

Table 1. Melting Points of Duplexes

duplex	residues at site of modification[a]	T_m (°C)[b]
15/**12**	A/T	68.5
9/**10**	-P-/-	61.5
9/**11**	-P-/Z	62.0
9/**12**	-P-/T	63.0
9/**13**	-P-/X	62.5
9/**14**	-P-/TTT	54.2

[a] See Scheme 3 for full sequences. [b] Defined as the maximum in the first derivative of the melting curve.

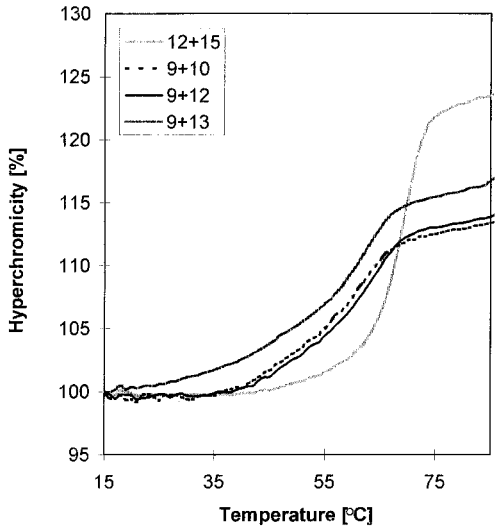

Figure 1. UV-melting curves of DNA/DNA and DNA/porphyrin−DNA duplexes. Changes of absorbance upon heating as monitored at 260 nm (1.3 μM in phosphate-buffered solution, 0.1 mM EDTA, pH 7.0).

401 nm, on the other hand, displayed a hyperchromicity of less than 20% between 30 °C and 80 °C, much like the nucleobase-absorption at 257 nm (Figure 2c). The maximum of this absorption shifted 4 nm to shorter wavelengths during melting, a change also observed for single stranded **9** upon heating (Figure 2d). The extensive changes in the Q-bands, however, were not observed in the single-stranded control (Figure 2b). Finally, it is noteworthy that the T_m determined from a hyperchomicity plot of the porphyrin band at 501 nm was similar to that determined at the DNA wavelength of 260 nm.

The structure of the porphyrin-containing duplex **9**/**12** was subsequently probed by CD-spectropolarimetry. At low temperatures, bands characteristic for B-DNA were observed (Figure 3). In fact, the spectrum did not show signs of a major structural distortion. The changes in the CD spectrum upon heating confirmed the results of the UV-melting study. A loss of elipticity typical for DNA undergoing a transition from the duplex state to random coil was observed (Figure 3). The melting temperature derived from these spectra is similar to that derived from the absorbance versus temperature profiles (see Supporting Information). Therefore, it was concluded that, while moderately lowering the thermal stability, the porphyrin does not prevent formation of a regular, Watson−Crick paired B-duplex.

This conclusion was confirmed in a footprinting assay monitored by MALDI-TOF mass spectrometry. The vulnerability of **9** toward degradation by nuclease S1 (EC 3.1.30.1), a single strand-specific nuclease that does not rapidly hydrolyze regular B-form DNA, was determined.

(12) While in the present case, an "inversion" occurs on the design level, a conceptually similar pyrrole inversion has been discussed for naturally occurring porphyrinogens; Franck, B. *Angew. Chem., Int. Ed. Engl.* **1982**, *21*, 343−353 and references therein.
(13) Honeybourne, C. L.; Jackson, J. T.; Simmonds, D. S.; Jones, O. T. G. *Tetrahedron* **1980**, *36*, 1833−1838.
(14) (a) Chong, R.; Clezy, P. S.; Liepa, A. J.; Nichol, A. W. *Aust. J. Chem.* **1969**, *22*, 229−237. (b) Paine, J. B. III, Woodward, R. B.; Dolphin, D. *J. Org. Chem.* **1976**, *41*, 2826−2835.
(15) Arsenault, G. P.; Bullock, E.; McDonald, S. F. *J. Am. Chem. Soc.* **1960**, *82*, 4384−4389.
(16) (a) Gunter, M. J.; Mander, L. N. *J. Org. Chem.* **1981**, *46*, 4792−4795. (b) Young, R.; Chang, C. K. *J. Am. Chem. Soc.* **1985**, *107*, 898−909.
(17) Richert, C.; Wessels, J. M.; Müller, M.; Kisters, M.; Benninghaus, T.; Goetz, A. E. *J. Med. Chem.* **1994**, *37*, 2797−2807.
(18) Kierzek, R.; Kopp, D. W.; Edmonds, M.; Caruthers, M. H. *Nucleic Acids Res.* **1986**, *14*, 4751−4764.

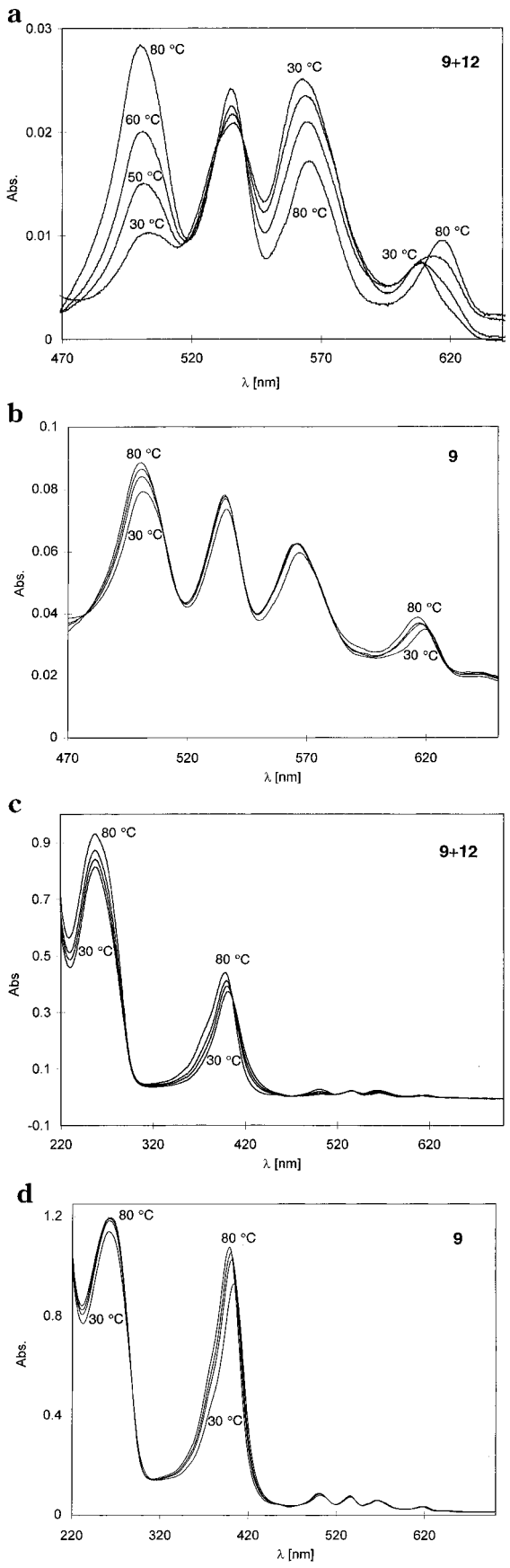

Figure 2. Changes in the UV−vis spectra of duplex **9**/**12** and single stranded **9** upon heating. Expansion of the Q-band region for **9**/**12** (a), and **9** (b); full spectra for **9**/**12** (c), and **9** (d); recorded in 100 mM NaCl, 10 mM K_2HPO_4/KH_2PO_4 buffer, 0.1 mM EDTA, pH 7.0.

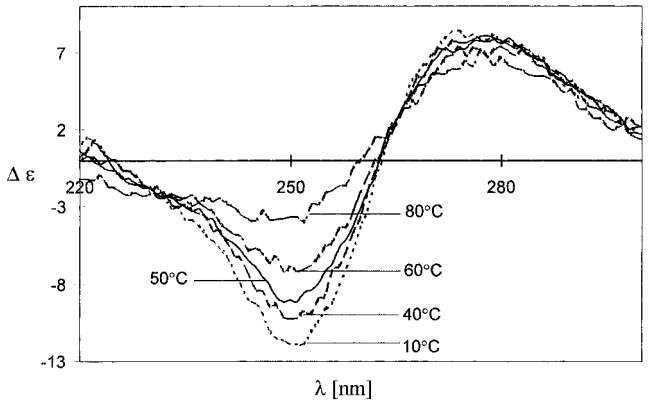

Figure 3. Changes in the circular dichroism spectrum of duplex **9**/**12** upon thermal denaturation (26 μM solution in 220 mM NaCl, 20 mM phosphate-buffer, pH 7.0).

The formation of fragments was measured under quantitative detection conditions, as previously reported.[19] In the present case, DNA dodecamer 5′-ACGTCAGTTAGC-3′ was added to the matrix as internal standard, and relative peaks intensities (analyte/internal standard) were measured for the fragments generated by the nuclease reaction. Fragments originating from attack of the nuclease at 12 of the 17 phosphodiester positions in **9** could be detected (Figure 4). These constitute the sites where the accessibility toward nuclease attack was determined. Besides **9**/**12**, the duplex **9**/**10** and the mixture of noncomplementary strands **9** and **15** were subjected to the nuclease attack. The latter served as a control to determine the rate of fragment formation for "naked", single stranded **9** at the same overall nucleotide concentration. As expected for intact double helixes, the rate of hydrolysis was reduced for **9**/**12** and **9**/**10** compared to the mixture of **9** and **15**. The only exceptions to this observation were the cleavage sites adjacent to the porphyrin, where no statistically significant differences were detected. A "snapshot" of the relative fragment intensities observed after 20 min reaction time are shown in Figure 4. This representation was chosen, as kinetic analyses of the fragment formation reactions were complicated by concurrent secondary cleavage reactions whose contribution was difficult to determine in some cases. Independent of the moderate sequence specificity of the enzyme and gradual differences between individual cleavage sites, the nuclease resistance established that the complementary DNA regions 5′ and 3′ to the porphyrin/T site both form Watson−Crick duplexes. Interestingly, phosphodiesters in **9** were on average less well protected in the duplex with heptadecamer **10** than in the duplex with octadecamer **12**, where a thymidine residue is located opposite the porphyrin. This indicates that structural differences between the two duplexes are more pronounced than expected based on UV melting points (Table 1).

Fluorescence spectra provided additional evidence for interactions between the embedded porphyrin and the neighboring nucleic acids. Compared to porphyrin dialcohol **6** in methanol, the intensity of the fluorescence maximum of oligonucleotide hybrid **9** in aqueous buffer was reduced 8-fold (Figure 5 and Supporting Information). The wavelength of the main maximum was the

(19) Sarracino, D.; Richert, C. *Bioorg. Med. Chem. Lett.* **1996**, *6*, 2543−2548.

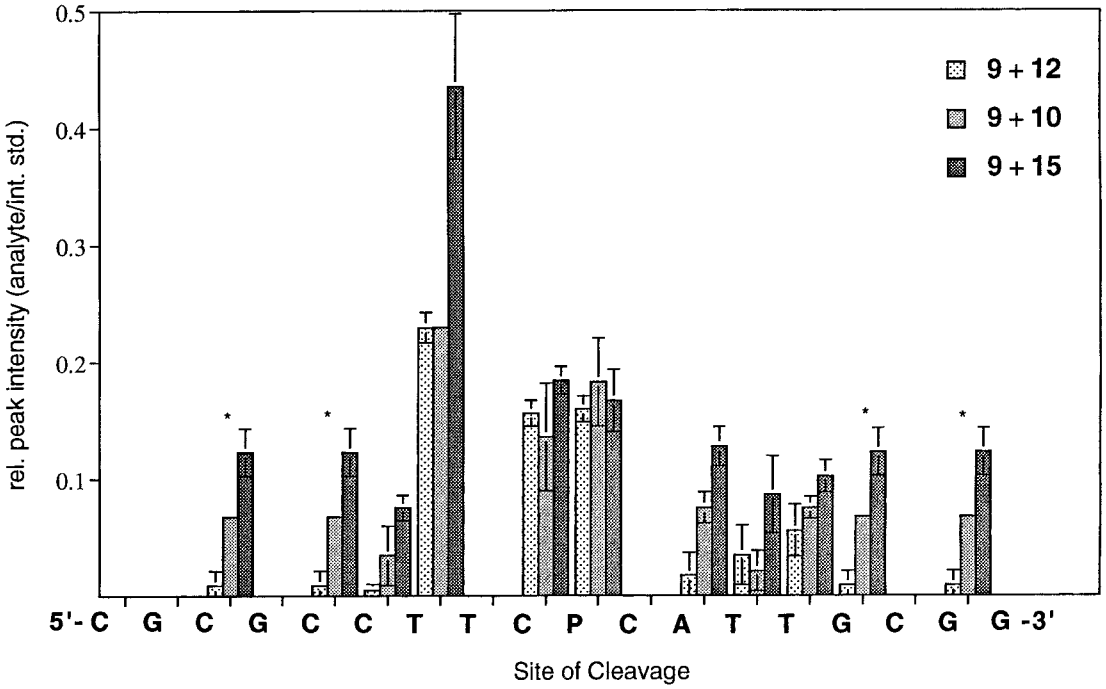

Figure 4. Comparison of nuclease sensitivity of porphyrin−DNA oligomer **9** when complexed with **12**, **10**, or mixed with noncomplementary octadecamer **15**. Relative peak intensities of fragments formed in the cleavage reaction with nuclease S1 (EC 3.1.30.1), as detected in MALDI-TOF mass spectra acquired under conditions yielding quantitative concentration−intensity relationships.[19] Relative peak intensities were measured after 20 min degradation time with 0.1 units/μL nuclease S1 acting on 24 μM **9** and 25 μM **10**, **12**, or **15** at pH 5.6 and 37 °C. Bars represent the mean relative peak intensities from three independent experiments, error bars are one standard deviation. Only fragments formed with a sufficiently fast rate and with suitable desorption properties could be detected. Bars marked with an asterisk indicate peaks whose assignment to a phosphodiester cleavage site was ambiguous. See Supporting Information for a typical spectrum.

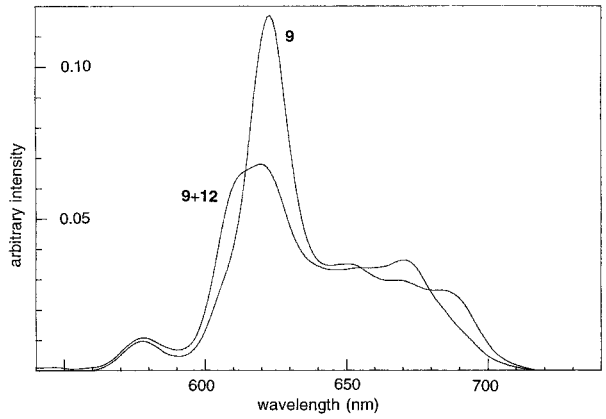

Figure 5. Fluorescence spectra of porphyrin−DNA hybrid **9** in single stranded state and complexed with complementary strand **12**. Spectra of 0.3 μM solutions (E_{403} < 0.05) in 148 mM NaCl, 15 mM phosphate buffer, pH 7.0, 20 °C; excitation wavelength 396 nm.

same within ±2 nm, but the order of intensity of the vibrational bands was reversed. While the longer wavelength vibrational bands of **9** were less intense than those at shorter wavelength, the longest wavelength band observed for **6** in methanol (685 nm) was the most intense. A ca. 20% increase in fluorescence was observed for **9** when the ionic strength was raised from 10 mM to 200 mM, but the appearance of the spectrum remained unchanged (not shown). More pronounced changes were induced when **9** was annealed to **12**, i.e upon the transition from single- to double-stranded state (Figure 5). A net quenching of porphyrin fluorescence was accompanied by the appearance of a shoulder on the main maximum and hypsochromic shifts and intensity changes for the now partly indistinguishable vibrational bands. This, together with the strongly temperature-dependent UV−vis spectra (Figure 2) indicated that the porphyrin does, in fact, interact with the nucleic acids, and that the interaction is more extensive in the double- than in the single-stranded state.

To obtain a first, qualitative impression of structural details of the interactions between porphyrin and the duplex DNA, one-dimensional NMR spectra of **9** annealed to **12** were acquired in buffered D_2O solution (Figure 6). While the analysis of the more crowded high-field region of the spectrum must await the acquisition of two-dimensional spectra, the low field region could be interpreted, as it contained only a small number of resonances, originating most probably from the meso-protons of the porphyrin. These resonances were sharp and similar in chemical shift at 70 °C, as expected for a porphyrin ring tumbling in solution. Lowering of the temperature led to a broadening of these signals and a shift of some but not all of these resonances to higher field. This may be indicative of a partial intercalation of the porphyrin ring in the forming DNA duplex. Line broadening effects and shifts to higher field are known for aromatic compounds whose intercalation is firmly established.[20] More than four resonances were observed at 50 °C, where a partial dissociation of the duplex is expected. The chemical shifts observed only at this partially melted stage point toward additional stacking modes of the porphyrin that require dissociation of some portion of the DNA duplex. Peaks of similar chemical shift but different intensity

(20) See e.g.: Greguric, I.; Aldrich-Wright, J. R.; Collins, J. G. *J. Am. Chem. Soc.* **1997**, *119*, 3621−3622.

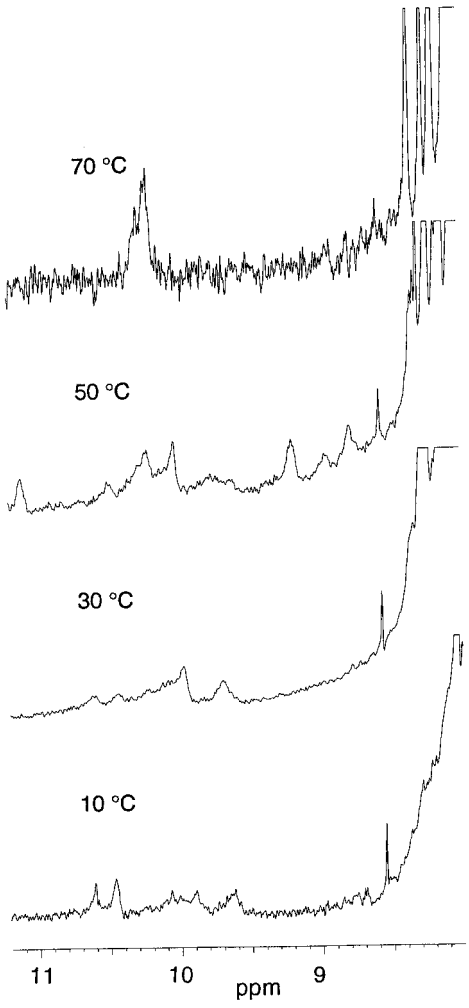

Figure 6. Changes in the ^{1}H NMR spectrum of **9** (50 μM) complexed with **12** (60 μM) upon heating. Expansion of the spectral region containing the signals of the meso protons of the porphyrin; 500 MHz, D_2O, 120 mM NaCl, 12 mM phosphate buffer, pH 7.0. Differences in signal-to-noise ratios are due to different acquisition times needed for unambiguous detection of peaks.

were detected at 30 °C and 10 °C, indicating that the porphyrin may be in an equilibrium between two states whose population changes as a function of temperature.

Discussion

One goal of the present study was to provide a building block for incorporation of a porphyrin at any given position of double stranded DNA. As such, phosphoramidite **1** may have a number of applications. Porphyrin−, metalloporphyrin−, and porphyrinoid−DNA hybrids appended to one terminus of an oligodeoxynucleotide can act as artificial, site-specific nucleases.[21] Except for a texaphyrin phosphoramidite reported after completion of our study,[22] such hybrids were not prepared via standard phosphoramidite chemistry.[23] Phosphoramidite **1** allows for automated solid-phase syntheses of porphyrin-hybrids without a bifunctional linker. The porphyrin is incorporated in the nucleotide chain via short tethers, allowing a very precise delivery to a target site. Porphyrin-bearing double stranded DNA oligomers with "sticky ends" may be ligated into plasmids and other multigene duplexes. These would be without major structural disturbances, but would bear the porphyrin photosensitizer at a single, distinct site. Thus, "point-mutated" plasmids, ideal models for studying photosensitization-induced damage in complex systems, may be prepared. Extension to metalloporphyrins can be envisioned via a metalation step performed after porphyrin assembly and prior to the tritylation of **6**.

Other applications could make use of spectroscopic properties of the embedded porphyrin. The change in fluorescence upon duplex formation, for example, could be used to detect transitions in nucleic acids.[24] Porphyrins, when excited at the Sôret maximum, offer a large Stokes shift, an advantage for detection in biological systems which often give strong background signal.[25] Provided that attempts to perform NMR-based structure elucidation will be successful, the much-debated[26] question of the efficiency of electron transfer through DNA[27] may be studied with porphyrin−DNA hybrids as structurally well-defined model systems.

The embedded porphyrin does not bear the positively charged aryl groups that dominate the interactions of the known, xenobiotic nucleic acid-binding porphyrins.[9] It therefore offers an opportunity to study the intercalative properties of porphyrin itself without complications from template-directed aggregation of porphyrin rings.[6] The propyloxy tethers are expected to give the porphyrin the conformational mobility required to interact with the DNA or to flip out into solution. A possible equilibration between these two states, for which our experiments set the stage, could also help to better understand the recognition chemistry of nucleic acids, as the alkylporphyrin is an archetypal hydrophobic aromatic macrocycle without hydrogen bonding capabilities, whose binding may only be driven by hydrophobic effects, van der Waals interactions, and dipole−dipole interactions.

From our preliminary study, we conclude that the porphyrin does interact with DNA, both in single- and double-stranded state, rather than flipping out into solution. This is evident from the changes in absorbance,

(21) (a) Le Doan, T.; Perrouault, L.; Hélène, C. *Biochemistry* **1986**, *25*, 6736−6739. (b) Le Doan, T. Perrouault, L.; Chassignol, M.; Thoung, N. T.; Hélène, C. *Nucleic Acids Res.* **1987**, *15*, 8643−8659. (c) Fedorova, O. S.; Savitskii, A. P.; Shoikhet, K. G.; Ponomarev, G. V. *FEBS Lett.* **1990**, *259*, 335−337. (d) Le Doan, T.; Praseuth, D.; Perrouault, L.; Chassignol, M.; Thoung, N. T.; Hélène, C. *Bioconjugate Chem.* **1990**, *1*, 108−113. (e) Boutorine, A. S.; Le Doan, T.; Battioni, J. P.; Mansuy, D.; Dupré, Hélène, C. *Bioconjugate Chem.* **1990**, *1*, 350−356. (f) Pitié, M.; Casas, C.; Lacey, C. J.; Pratviel, G.; Bernadou, J.; Meunier, B. *Angew. Chem., Int. Ed. Engl.* **1993**, *32*, 557−559. (g) Casas, C.; Lacey, C. J.; Meunier, B. *Bioconjugate Chem.* **1993**, *4*, 366−371. (h) Frovola, E.; Fedorova, O. S.; Knorre, D. G. *Biochimie* **1993**, *75*, 5−12. (i) Mastruzzo, L.; Woisard, A.; Ma, D. D. F.; Rizzarelli, E.; Favre, A.; Le Doan, T. *Photochem. Photbiol.* **1994**, *60*, 316−322. (j) Magda, D.; Wright, M.; Miller, R. A.; Sessler, J. L.; Sansom, P. I. *J. Am. Chem. Soc.* **1995**, *117*, 3629−3630. (k) Mestre, B.; Pratviel, G.; Meunier, B. *Bioconjugate Chem.* **1995**, *6*, 466−472. (l) Boutorine, A. S.; Brault, D.; Takasugi, M.; Delgado, O.; Hélène, C. *J. Am. Chem. Soc.* **1996**, *118*, 9−9476.

(22) Magda, D.; Crofts, S.; Lin, A.; Miles, D.; Wright, M.; Sessler, J. L. *J. Am. Chem. Soc.* **1997**, *119*, 2293−2294.

(23) (a) Sessler, J. L.; Sansom, P. I.; Kral, V.; O'Connor, D.; Iverson, B. L. *J. Am. Chem. Soc.* **1996**, *118*, 12322−12330. (b) Li H.; Fedorova, O. S.; Trumble, W. R.; Fletcher, T. R.; Czuchajowski, L. *Bioconjugate Chem.* **1997**, *8*, 49−56.

(24) (a) Wiederholt, K.; Rajur, S. B.; Giuliano, J. J.; O'Donnell, M. J.; McLaughlin, L. W. *J. Am. Chem. Soc.* **1996**, *118*, 7055−7062. (b) Wiederholt, K.; Rajur, S. B.; McLaughlin L. W. *Bioconjugate Chem.* **1997**, *8*, 119−126.

(25) See e.g., Leunig, M.; Richert, C.; Gamarra, F.; Lumper, W.; Vogel, E.; Jocham, D.; Goetz, A. E. *Br. J. Cancer* **1993**,*68*, 225−234.

(26) (a) Wilson, E. K. *Chem. Eng. News* **1997**, *75*, 33−39. (b) Beratan, D. N.; Piyadarshy, S.; Risser, S. M. *Chem. Biol.* **1997**, *4*, 3−8.

(27) Murphy, C. J.; Arkin, M. R.; Jenkins, Y.; Ghatlia, N. D.; Bossman, S. H.; Turro, N. J.; Barton, J. K. *Science* **1993**, *262*, 1025−1029.

fluorescence, and NMR properties of the porphyrin that accompany duplex melting. The thermal stability of the duplexes is lower than that of the unmodified control duplex, indicating that the structural perturbations are not fully compensated for by favorable interactions between "ligand" and DNA. It is known that hydrophobic molecules appended to one terminus of an oligonucleotide via a ribose tether can increase the thermal stability of duplexes. In this situation of minimal structural disturbance, ΔT_ms of +7 °C and +23 °C have been measured for a "dangling" benzene residue and its pyrene counterpart, respectively.[28] A 5-nitroindole moiety replacing any of the four nucleobases in DNA is less destabilizing than the corresponding nitropyrrole replacement with less hydrophobic surface area.[29] A non-ribose-tethered sapphyrin moiety, on the other hand gives a ΔT_m of only +3 °C.[23a] For the embedded porphyrin, the hydrophobic effects could be larger than in the latter case, as the porphyrin can get van der Waals contact with nucleobases on both of its faces. Release of bound water molecules would be substantial in this case. Therefore, one could have expected a stronger stabilization of the duplex than seen for the "end-on" stacking aromatics, if unfavorable contacts introduced by the linker and a possible disruption of the spine of hydration were of little energetic consequence. This argument, of course, only holds for the duplex **9**/**10**, where the porphyrin can intercalate in a duplex of two heptadecamers. In the other duplexes, the porphyrin has to flip out the nucleobase of the opposite strand in order to achieve full intercalation.

Duplex **9**/**10** melted at a slightly lower temperature than **9**/**12**, where the porphyrin faces an unpaired thymidine residue in the complementary strand, and **9**/**10** was also more quickly hydrolyzed by nuclease S1 than **9**/**12**. The stability of the latter duplex containing a porphyrin−thymidine "pair" may be compared with that of other backbone-modified oligonucleotides. Melting points of modified duplexes have been determined in large number for oligonucleotides with a potential to become nuclease resistant antisense inhibitors of gene expression.[30] Depletion of the melting point by several degrees per modification is typical even for seemingly minor backbone modifications, such as the replacement of one nonbridging phosphate oxygen by a sulfur atom[31] or a methyl group.[32] More extensive modifications, such as replacement of one phosphodiester with an isosteric nonionic linker and concomitant addition of a 2′-hydroxyl group to the deoxyribose, can depress the melting point of a DNA decamer duplex by 16 °C,[33] i.e., much more than observed for the porphyrin modification. Incorporation of a single acyclic nucleoside, which induces an entropic disadvantage for duplex formation similar to that of the flexibly tethered porphyrin, can depress the melting point of DNA duplexes by as much as 15 °C.[34] Compared to acyclic residues, the porphyrin "residue" is further handicapped, as it does not have the capability to form Watson−Crick base pairs. Assuming additive effects, 10−20 °C "expected melting point depression" could be added to the $-\Delta T_m$ expected based on the flexibility of the tether. Taken together, these considerations lead us to assume that the depression of the melting temperature observed for **9**/**12** versus **15**/**12** is moderate, and a substantial attractive interaction between porphyrin ring and DNA seems likely. This is confirmed by the much lower melting point of the duplex with **14**, whose additional nucleotides at the site of the porphyrin modification make a conformation with tight interactions difficult.

The higher stability of the duplex with a thymine residue facing the porphyrin could reflect the fact that this nucleobase is most easily flipped out. If so, full intercalation of the porphyrin would seem likely. The spreading of the NMR resonances tentatively assigned to the *meso*-protons of the porphyrin does not favor this interpretation, however. Instead, a partial intercalation seems more likely. A more precise structural picture is expected to emerge from multidimensional NMR experiments and molecular dynamics. The complex **9**/**12** could lead to such a picture as, contrary to untethered tetraarylpophyrins,[35] the specificity of the interactions gives observable resonances for the porphyrin. The observation that NMR and UV melting occurs at similar temperatures, despite a higher concentration in the NMR experiment, is in agreement with findings for other modified DNA duplexes, whose imino resonances were monitored.[36]

Our alkylporphyrin has substituents similar to those found in the porphyrins that play pivotal roles in today's metabolism. Recently, RNA[37] and DNA[38] sequences have been discovered that bind similar porphyrins and catalyze their transformation. One may speculate that the "RNA world"[39] of prebiotic evolution could have recruited porphyrins[40] as cofactors for as yet unknown ribozymes.[41] With porphyrin building block **1**, suitable for standard solid phase phosphoramidite chain assembly of porphyrin−DNA and porphyrin−RNA sequences, libraries of porphyrin−nucleic acid hybrids can be synthesized and

(28) (a) Guckian, K. M.; Schweitzer, B. A.; Ren, R. X.-F.; Sheils, C. J.; Paris, P. L.; Tahmassebi, D. C.; Kool,. E. T. *J. Am. Chem. Soc.* **1996**, *118*, 8182−8283. (b) Ren, R. X.-F.; Chaudhuri, N. C.; Paris, P. L.; Rumney VI, S.; Kool, E. T. *J. Am. Chem. Soc.* **1996**, *118*, 7671−7678.
(29) Loakes, D.; Brown, D. M. *Nucleic Acids Res.* **1994**, *22*, 4039−4043.
(30) (a) Uhlmann, E.; Peyman, A. *Chem. Rev. (Washington, D.C.)* **1990**, *90*, 544−584. (b) Milligan, J. F.; Matteucci, M. D.; Martin, J. C. *J. Med. Chem.* **1993**, *36*, 1923−1937. (c) Hunziker, J.; Leumann, C. In *Modern Synthetic Methods 1995*: Ernst, B.; Leumann, C. Eds.; Verlag Helvetica Chimica Acta: Basel, 1995; pp 333−417. (d) Sanghvi, Y. S.; Dan Cook, P. In *Carbohydrate Modifications in Antisense Research*; Saghvi, Y. S., Cook, P. D., Eds.; ACS Symposium Series: Washington, DC, 1994; pp 1−23.
(31) (a) Eckstein, F. *Angew. Chem.* **1975**, *87*, 179−185; *Angew. Chem., Int. Ed. Engl.* **1975**, *14*, 160−166. (b) Stein, C. A.; Subasinghe, C.; Shinozuka, K.; Cohen, J. *Nucleic Acids Res.* **1988**, *16*, 3209−3221.
(32) (a) Miller, P. S.; McFarland, K. B.; Jayaraman, K.; Ts'o, P. O. P. *Biochemistry* **1981**, *20*, 1878−1880. (b) Sarin, P. S.; Agarwal, S.; Civeira, M. P.; Goodchild, J.; Ikeuchi, T.; Zamecnik, P. C. *Proc. Natl. Acad. Sci. U.S.A.* **1988**, *85*, 7448−7451.
(33) Baeschlin, D. K.; Hyrup, B.; Benner, S. A.; Richert, C. *J. Org. Chem.* **1996**, *61*, 7620−7626.
(34) (a) Schneider, K. C.; Benner, S. A. *J. Am. Chem. Soc.* **1990**, *112*, 453−455. (b) Nielsen, P.; Kirpekar, F.; Wengel, J. *Nucleic Acids Res.* **1994**, *22*, 703−710.
(35) Marzilli, L. G.; Banvill, D. L.; Zon, G.; Wilson, W. D. *J. Am. Chem. Soc.* **1986**, *108*, 4188−4192.
(36) Gao, X.; Brown, F. K.; Jeffs, P.; Bischofsberger, N.; Lin, K.-Y.; Pipe, A. J.; Noble, S. A. *Biochemistry* **1992**, *31*, 6228−6236.
(37) Conn, M. M.; Prudent, J. R.; Schultz, P. G. *J. Am. Chem. Soc.* **1996**, *118*, 7012−7013.
(38) (a) Li, Y.; Geyer, C. R., Sen, D. *Biochemistry* **1996**, *35*, 6911−6922. (b) Li Y.; Sen, A. *Nature Struct. Biol.* **1996**, *3*, 743−747.
(39) (a) Gilbert, W. *Nature* **1986**, *319*, 618. (b) Benner, S. A.; Ellington, A. D.; Tauer, A. *Proc. Natl Acad. Sci. USA* **1989**, *86*, 7054−7058. (c) Gesteland, R. F., Atkins, J. F., Eds. *The RNA World*; Cold Spring Harbor Press: Cold Spring Harbor, 1993.
(40) Scott, A. I. *Tetrahedron Lett.* **1997**, *38*, 4961−4964.
(41) Breaker, R. R.; Joyce, G. F. *J. Mol. Evol.* **1995**, *40*, 551−559.
(42) Berlin, K.; Jain, R. K.; Tetzlaff, C.; Steinbeck, C.; Richert, C. *Chem. Biol.* **1997**, *4*, 63−77.

subjected to in vitro selection, e.g. via monitored selection experiments.[42]

Conclusion

Presented here is a synthesis of porphyrin−DNA hybrids via automated chain assembly using the phosphoramidite protocol. Physicochemical characterization of porphyrin-bearing oligodeoxynucleotides as single strands and complexed with complementary strands indicates that the porphyrin ring does interact with the nucleic acids. This interaction seems more extensive in double- than in single-stranded state of the nucleic acids. It is sequence-dependent, and, judged by the UV−vis spectrum, does not seem to be similar to the interactions of cationic tetraarylporphyrins.[1−3,43] These and the findings on nonstandard, G-rich DNA sequences[38] lead us to conclude that a rich porphyrin−nucleic acid recognition chemistry exists beyond that involving the known cationic tetraarylporphyrin nucleic acid binders.

Experimental Section

General. Acetonitrile, cyclohexane, ethanol, ethyl acetate, pyridine, and tetrahydrofuran were from Fisher Scientific, benzene, and dichloromethane were from VWR (EM brand), methanol was from Baker, and dimethylformamide was from Fluka. Phosphate-buffered saline solution (PBS) was made up from NaCl (8 g, 136 mmol), $K_2HPO_4 \cdot 3H_2O$ (1.6 g, 7 mmol), KH_2PO_4 (0.272 g, 2 mmol), KCl (0.2 g, 3 mmol), and deionized water (1 L total volume). Analytical thin-layer chromatography was performed on Whatman PE SILG/UV 250 μm layer precoated silica gel plates, and compounds were visualized with UV light or staining with cerium(IV) sulfate/phosphomolybdic acid/H_2SO_4 (concentrated) and subsequent heating. Column chromatography was performed on Merck silica gel grade 9385, 0.040−0.063 mm mesh, 60 Å. Eluant mixtures for chromatography are expressed as ratios of volumes. NMR spectra at 500 MHz were recorded on a spectrometer custom-designed at the Francis Bitter Magnet Laboratory, Massachusetts Institute of Technology, Cambridge, MA. Spectra were processed using GIFA.[44] High-resolution mass spectra were acquired by the Mass Spectrometric Facility, Chemical Laboratories, Harvard University, with an error limit of ±5 ppm.

Diethyl 3,3′-Bis(3-hydroxypropyl)-4,4′-dimethyl-2,2′-dipyrrylmethane-5,5′-dicarboxylate (4). Diethyl 3,3′-bis-[2-(methoxycarbonyl)ethyl]-3,3′-dimethyl-2,2′-dipyrrylmethane-5,5′-dicarboxylate (**2**) (21.3 g, 43.4 mmol) was dissolved in dry THF (100 mL) under argon, and borane−THF complex (1.0 M in THF, 180 mL, 180 mmol) was added dropwise over 15 min. The reaction mixture was stirred overnight at room temperature. Methanol (20 mL) was added, and the solvent was evaporated under reduced pressure to provide a white solid that was recrystallized from ethanol. Yield: 12.8 g (29.5 mmol, 68%), mp 134 °C. ^{1}H NMR (300 MHz, $CDCl_3$) δ = 1.25 (t, 6H), 1.73 (quint, 4H), 2.19 (s, 6H), 2.62 (t, 4H), 3.00 (s br, 2H), 3.60 (t, 4H), 3.77 (s, 2H), 4.18 (q, 4H), 10.02 (s br, 2H). ^{13}C NMR (75 MHz, $CDCl_3$) δ = 10.9, 14.3, 19.7, 22.2, 31.7, 59.5, 61.3, 118.0, 120.3, 126.8, 131.1, 162.3. MS (EI, 70 eV) *m*/*z* (%) = 434 ($M^{+\bullet}$, 100), 375 (61), 329 (40), 209 (31), 167 (70), 134 (76). HRMS (FAB) calcd for $C_{23}H_{34}N_2O_6$ [$M^{+\cdot}$] 434.2417, found 434.2431.

3,3′-Bis(3-hydroxypropyl)-4,4′-dimethyl-2,2′-dipyrrylmethane (5). Diethyl 3,3′-bis(3-hydroxypropyl)-4,4′-dimethyl-2,2′-dipyrrylmethane-5,5′-dicarboxylate (**4**) (4 g, 9.2 mmol) was suspended in ethanol (80 mL), and a solution of sodium hydroxide (2 g, 50 mmol) in water (30 mL) was added. The reaction mixture was heated under reflux for 5 h. The ethanol was distilled off under reduced pressure, and the residue was diluted with water (40 mL). Hydrazine monohydrate (6 mL) was added, and the solution was refluxed for 15 h. A pale brown-yellow oil formed on the surface. Additional hydrazine hydrate (4 mL) was added and the reaction mixture heated under reflux for another 15 h. The brown, highly viscous oil was separated, washed several times with water, and dried in vacuo overnight. Yield: 1.95 g (6.7 mmol, 73%) of the highly air-sensitive target compound. ^{1}H NMR (300 MHz, $CDCl_3$) δ = 1.72 (quint, 4H), 1.98 (s, 6H), 2.51 (t, 4H), 3.60 (t, 4H), 3.78 (s, 2H), 6.32 (s, 2H), 8.05 (s br, 2H). ^{13}C NMR (75 MHz, $CDCl_3$) δ = 10.4, 20.6, 22.6, 33.1, 62.6, 114.2, 117.4, 117.8, 125.8. MS (EI, 70 eV) *m*/*z* (%) = 290 ($M^{+\bullet}$, 100), 231 (93), 108 (79), 95 (55).

8,12-Diethyl-2,18-bis(3-hydroxypropyl)-3,7,13,17-tetramethylporphyrin (6). 3,3′-Diethyl-4,4′-dimethyl-2,2′-dipyrrylmethane-5,5′-dicarboxaldehyde (**3**) (286 mg, 1 mmol) and 3,3′-bis(3-hydroxypropyl)-4,4′-dimethyl-2,2′-dipyrrylmethane (**5**) (290 mg, 1 mmol) were dissolved in methanol (150 mL). The solution was degassed with an argon stream and the flask protected from light. *p*-Toluenesulfonic acid (0.3 g, 1.6 mmol) was added, and the reaction mixture was stirred for 5 h under exclusion of oxygen and light. *p*-Chloranil (0.4 g, 1.6 mmol) was added, and the solution was stirred overnight. The solvent was evaporated and the red-brown residue was purified by flash column chromatography on silica (ethyl acetate/dichloromethane 1:2, then THF/dichloromethane/water 100:100:1). The product-containing fractions were concentrated to 100 mL, and the porphyrin was precipitated with cyclohexane. The purple solid was filtered off to yield 187 mg (347 mmol, 35%) of the desired product as a red-brown microcrystalline solid: mp > 250 °C. ^{1}H NMR (300 MHz, $CDCl_3$/methanol-d_4, 3:1) δ = 1.72 (t, 6H), 2.38 (quint, 4H), 3.64 (s, 12H), 3.82 (t, 4H), 3.9−4.15 (m, 8H), 9.96 (s, 1H), 9.98 (s, 2H), 10.12 (s, 1H). ^{13}C NMR (75 MHz, $CDCl_3$/methanol-d_4, 3:1) δ = 11.1, 11.2, 17.4, 19.5, 20.3, 35.2, 61.5, 95.9, 96.0 96.2, quarternary carbons not detectable due to low solubility. UV, CH_2Cl_2:MeOH, (9:1) λ_{max} (ϵ) 269 (10,400); 396 (143,000); 497 (12,000); 533 (8,800); 566 (5,900); 618 (4,100). HRMS (FAB) calcd for $C_{34}H_{43}O_2N_4$ [M + H]$^+$ 539.3386, found 539.3389.

8,12-Diethyl-18-(3-hydroxypropyl)-2-{3-[bis(4-methoxyphenyl)phenylmethoxy]propyl}-3,7,13,17-tetramethylporphyrin (7). 8,12-Diethyl-2,18-bis(3-hydroxypropyl)-3,7,13,17-tetramethylporphyrin (**6**) (100 mg, 186 μmol) was coevaporated with pyridine (5 mL). Molecular sieves (0.5 g, 4 Å) and 4-(dimethylamino)pyridine (2 mg, 16 μmol) were added. The mixture was dried in high vacuum at 50 °C for 1 h, and the flask was vented with argon. The educt was suspended in pyridine (6 mL) and benzene (6 mL), and triethylamine (100 μL, 720 μmol) was added. The reaction was heated under reflux for 15 min to give a dark red solution before 4,4′-dimethoxytrityl chloride (70 mg, 207 μmol) was added in one portion. The reaction mixture was heated under reflux for 16 h under argon. Methanol (5 mL) was added, and the solvents were evaporated under reduced pressure. The residue was chromatographed on silica with dichloromethane/ethyl acetate/triethylamine, 90:10:1, to yield the title compound and with THF to recover unreacted starting material (35 mg, 65 μmol). Yield: 38 mg (45 μmol, 37% based on recovered starting material) of a red-brown, shiny microcrystalline solid. ^{1}H NMR (300 MHz, $CDCl_3$) δ = −3.83 (s br, 2H), 1.82 (t, 6H), 2.42, 2.52 (2 quint, 4H), 3.41 (t, 2H), 3.48−3.53 (4s, 12H), 3.73 (br t), 4.00−4.18 (m, 8H), 6.65 (d, 4H), 7.12 (t, 1H), 7.21 (t, 2H), 7.31 (d, 4H), 7.50 (d, 2H), 9.99−10.08 (4s, 4H). ^{13}C NMR (75 MHz, $CDCl_3$) δ = 11.5, 11.7, 17.7, 19.8, 22.4, 23.6, 33.6, 35.4, 54.9, 62.1, 63.6, 86.0, 96.1, 96.3, 112.9, 126.6, 127.7, 128.2, 130.0, 134.9, 135.1, 135.3, 135.5, 136.6, 139.9, 142.1, 145.4, 158.3. UV−vis (CH_2Cl_2, qualitative) λ_{max} = 397 (100%), 497 (8.4%), 530 (6.0%), 566 (3.8%), 619 (2.9%), 648 nm (1.2%). HRMS (FAB) calcd for $C_{55}H_{61}O_4N_4$ [M + H]$^+$ 841.4701, found 841.4693.

(43) Chaires, J. B. *Biophys. Chem.* **1990**, *35*, 191−202.
(44) Delsuc, M. A. In *Maximum Entropy and Bayesian Methods*; Skilling, J., Ed.; Kluwer Academic: Dordrecht, The Netherlands: 1989; pp 285−290.

8,12-Diethyl-18-(3-hydroxypropyl)-2-{3-[bis(4-methoxyphenyl)phenylmethoxy]propyl}-3,7,13,17-tetramethylporphyrin Cyanoethyl (Diisopropylamino)phosphoramidite (1). DMT-porphyrin (**7**) (100 mg, 120 μmol), diisopropylammonium tetrazolide (20 mg, 120 μmol), and molecular sieves (0.1 g, 4 Å) were dried in vacuo at 60 °C for 10 min. The flask was vented with argon, and dry acetonitrile (1.6 mL) and dry DMF (250 μL) were added under positive argon pressure. 2-Cyanoethyl tetraisopropylphosphoramidite (80 μL, 250 μmol) was added, followed by gentle heating, leading to a slow dissolution of the educt. The reaction mixture was stirred for 16 h at room temperature under exclusion of moisture and light. The reaction mixture was cooled to 5 °C and filtered and the filtrate diluted with dry acetonitrile (3 mL). After a few minutes of stirring, a brown-orange precipitate appeared. After another 30 min of stirring, the precipitate was filtered off, washed with a small amount of cold acetonitrile, and dried in vacuo. Yield 90 mg (87.4 μmol, 73%). The title compound is stable under argon at −20 °C. It rapidly decomposes in dichloromethane solution in the presence of just a trace of water. LD-MS (matrix-free conditions) calcd for $C_{64}H_{78}N_6O_5P$ [$M^{\cdot+}$] 1041.6, found 1041.6.

Synthesis of Oligonucleotides. Oligonucleotides and porphyrin-bearing oligonucleotides were synthesized on 1.0 μmol scale on an ABI 381A automatic synthesizer, system software version 1.5. Phosphoramidites for the naturally occurring nucleotides (dA^{Bz}), (dC^{Bz}), (dG^{DMF}), and (dT) were used as received from ABI − Perkin-Elmer. Oligonucleotide library **13** was prepared using an equimolar mixture of the four phosporamidites in the 10th coupling reaction. The abasic phosphoramidite building block used for the synthesis of **11** was obtained from Glen Research (Sterlin, VA) and used without modifications. Unmodified DNA oligomers were synthesized using the protocol recommended by ABI. For the synthesis of porphyrin-bearing oligomers, an extended coupling time of 10 min was employed for building block **1**, which was dissolved in CH_2Cl_2/NEt_3 (500:1). Further, 10% CH_2Cl_2 was added to the tetrazole activator solution to prevent precipitation of the porphyrin. The yield for **1** was ca. 50%, based on trityl signals, with the most significant drop during coupling of the porphyrin building block. Oligonucleotides were purified by conventional RP-18 HPLC (Waters, Microsorb-MV, 5 μm, 100 Å, 250 × 4 mm) using a gradient of CH_3CN against 0.1 M triethylammonium acetate solution. Purification of **9** was similarly successful on Poly-Pak RP-cartridges (Glen Research), when elution of the product with 50% CH_3CN was used. Oligomers were >95% pure (unmodified strands), and ≥85% pure in the case of porphyrin-bearing oligomers, where lower desorption efficiencies accompanied by modest depurination and adduct formation made a more accurate determination of purity impossible. **8**, MALDI-MS, calcd for $C_{121}H_{153}N_{37}O_{56}P_9$ [M + H]$^+$ 3300.5 (average mass), found 3301 ± 3 (maximum of the unresolved isotope pattern), 1652 ± 2 [M + 2H]$^{2+}$. **9**, MALDI-MS, calcd for $C_{197}H_{251}N_{63}O_{107}P_{17}$ [M + H]$^+$ 5740.0 (average mass), found 5735 ± 5 (maximum of the unresolved isotope pattern), 2869 ± 3 [M + 2H]$^{2+}$.

UV Melting Experiments. Solutions of oligonucleotides (1.3 μM of each strand in phosphate-buffered solution; 100 mM NaCl, 10 mM K_2HPO_4/KH_2PO_4 buffer, 0.1 mM EDTA, pH 7.0) were heated to 95 °C, maintained at this temperature for 5 min, and then cooled slowly to 10 °C. Samples were then heated to 85 °C, and the absorption at 260 nm was measured at every 1 °C interval on an Aviv 14 DS spectrophotometer equipped with a thermostatable multicuvette holder. A brief temperature stabilization period preceded every data acquisition. Melting temperatures were determined as the maximum of the first derivative of the temperature versus absorbance profiles using Aviv V 4.1t software.

Nuclease Footprinting. Solutions of **9** (9 μL, 53 μM, 0.47 nmol) and either **10**, **12**, or **15** (10 μL, 50 μM, 0.50 nmol) were mixed and equilibrated to 37 °C for 15 min. A solution of nuclease S1 (3 μL, 0.8 units/μL, pH 5.6) in salt solution (0.5 M $(NH_4)_2SO_4$, 30 μM $ZnSO_4$) was added. Aliquots of 2 μL were removed after defined time periods and immediately mixed with a mixture of trihydroxyacetophenone (10 μL, 0.3 M in ethanol), diammonium citrate (4 μL, 0.1 M in water), and DNA oligomer 5′-ACGTCAGTTAGC-3′ (1 μL, 8.3 μM in water) at 0 °C. The dodecamer in this mixtures served as internal standard for quantitative evaluation of MALDI spectra. Data acquisition and evaluation parameters were similar to those previously reported for quantitative MALDI-TOF MS of oligonucleotides.[19] Briefly, aliquots of 0.75 μL of the matrix mixture were applied to MALDI target plates. Solvent evaporation at room temperature led to ring-shaped, semicrystalline matrix deposits. Six MALDI spectra of 50 laser shots each were acquired on a Bruker BIFLEX with a 1 GHz digitizer, delayed extraction, and a 2.1 m drift tube, using different regions of every matrix deposit at a laser fluence of ca. 100 μJ per shot, 2 Hz laser frequency, 2 mV preamplifier voltage, in negative delayed extraction mode at an extraction voltage of 20 kV (18.35 kV delayed extraction voltage). The linear sum of the six spectra was analyzed, and relative peak intensities (analyte/internal standard) were calculated. Every experiment was performed in triplicate.

Acknowledgment. The authors are grateful to C. Tetzlaff for solid phase syntheses, D. Sarracino for help with the footprinting assay, K. Wiederholt and L. McLaughlin for access to a UV-melting apparatus, C. Steinbeck, H. Gupta, and C. Turner for acquisition and processing of NMR data, and M. Uesugi and G. Verdine for access to the CD spectropolarimeter. The Center for Magnetic Resonance at the Francis Bitter Magnet Laboratory is supported by grant number RR00995, periods 19-22, from the National Center for Research Resources at the NIH. The authors thank Tufts University for support. K.B. was supported by a postdoctoral fellowship from the Stiftung Stipendien-Fonds des Verbandes der Chemischen Industrie, FRG, under the Post Doc-Stipendien VAA program.

Supporting Information Available: NMR spectra of **4**, **5**, **6**, and **7**, MALDI mass spectra of **8** and **9**, a CD melting curve for the duplex **9**/**12**, a typical mass spectrum from the footprinting study, selected kinetics of the fragment formation during nuclease degradation, and a fluorescence spectrum of **10** (10 pages). This material is contained in libraries on microfiche, immediately follows this article in the microfilm version of the journal, and can be ordered from the ACS; see any current masthead page for ordering information.

JO9718051